

Chapter N

Tectonic Modeling of Yucca Mountain

By Bob Janssen¹ and Geoffrey King¹

Contents

Abstract.....	2
Introduction	2
Cross-Sectional Models of Normal Fault Structures	2
Two-Dimensional Modeling of Dip-Slip Planar Faults Incorporating Buoyancy and Erosion and Deposition of Sediment.....	7
Two-Dimensional Yucca Mountain Models.....	7
Results from Planar Dip-Slip Modeling.....	11
Shear-Zone Modeling in Plan View.....	11
Boundary Conditions and Models of Yucca Mountain	11
A Model for Yucca Mountain Based on Observed Displacements	13
Conclusions	17
References Cited	17

Figures

1. Relief map and cross section of Yucca Mountain area	3
2. Cross section of model of normal fault structures	4
3. Simplified geologic map of Virgin Mountains	5
4. Schematic cross section of Virgin Mountains	6
5. Cross sections showing effects of changing modeling parameters	8
6. Two-dimensional cross-section models of Yucca Mountain	10
7. Map view of shear zone composed of rotating blocks	11
8. Simplified map of faults around Yucca Mountain, and map views of block-faulting models	12
9. Map views of three models showing effects of shear deformation on rotating blocks	13
10. Map showing simplified fault system used to generate a three-dimensional model for Yucca Mountain.....	14
11. Three-dimensional model diagrams showing deformation on faults at Yucca Mountain	15
12. Profiles of Yucca Mountain models and cross sections	16

[For table of abbreviations and conversions, click [here](#)]

¹Institut de Physique du Globe, 5, rue René Descartes,
6708 Strasbourg, Cedex, France.

Abstract

Mechanical and kinematic models have been developed for the Yucca Mountain region. The simple geometries that we use aim to show the relations between fault behavior at depth and features observed at or near the surface. For the cross-sectional models around Yucca Mountain we adopt planar normal faults throughout the brittle crust. Uplift and tilting of blocks are explained by isostatic effects. In plan view, oblique slip is explained using bookshelf-type models. These assume a set of subparallel faults situated in a region subjected to shear. The direction of shear is perpendicular to the strike of faults, a condition that minimizes internal deformation of fault-bounded blocks. Normal components of fault slip create topography. Estimates of the throw on faults are used to calculate the associated deformation field, including the flexural effects caused by the isostatic component as well as loading/unloading by deposition/erosion of sediments. In order to simulate the observed topography, a fault with an approximate throw of 3 kilometers must exist under Crater Flat, and normal faulting must exist outside the modeled Yucca Mountain area.

Introduction

In this report we use models of a kinematic and mechanical nature. Three types of models for Yucca Mountain are developed. Cross sections, plan-view models, and a three-dimensional model show the relations between slip on steeply dipping planar faults and the geologic structure observed at or near the surface. In the cross sections we show that deformation at Yucca Mountain can be modeled using steeply dipping planar faults. Isostatic adjustment causes uplift and rotation of fault-bounded blocks, eliminating the need for listric and detachment faulting to explain the tilt of blocks. The thickness of the brittle seismogenic crust in the Basin and Range province is about 12–15 km (Smith and Bruhn, 1984). In order to obtain feasible flexures, the effective elastic thickness has to be on the order of 2 km (Stein and others, 1988; King and Ellis, 1990).

In the plan-view models we adopt a bookshelf-type structure (Nur and others, 1986; McKenzie and Jackson, 1986) to explain the occurrence of oblique slip on normal faults in the Yucca Mountain region. This model assumes that subparallel faults are situated in an area that is subjected to shear. The direction of shear, which is perpendicular to the strike of faults, minimizes internal deformation of fault-bounded blocks but produces slip vectors that are oblique to strike on faults.

Normal faulting creates topography that can also be computed. Estimates of throw on faults are introduced into a model representing the approximate geometry of faulting around Yucca Mountain. The resulting model, which incorporates only simple planar faults cutting the brittle crust and mechanical properties consistent with the earthquake cycle, bears a striking similarity to topography of the area.

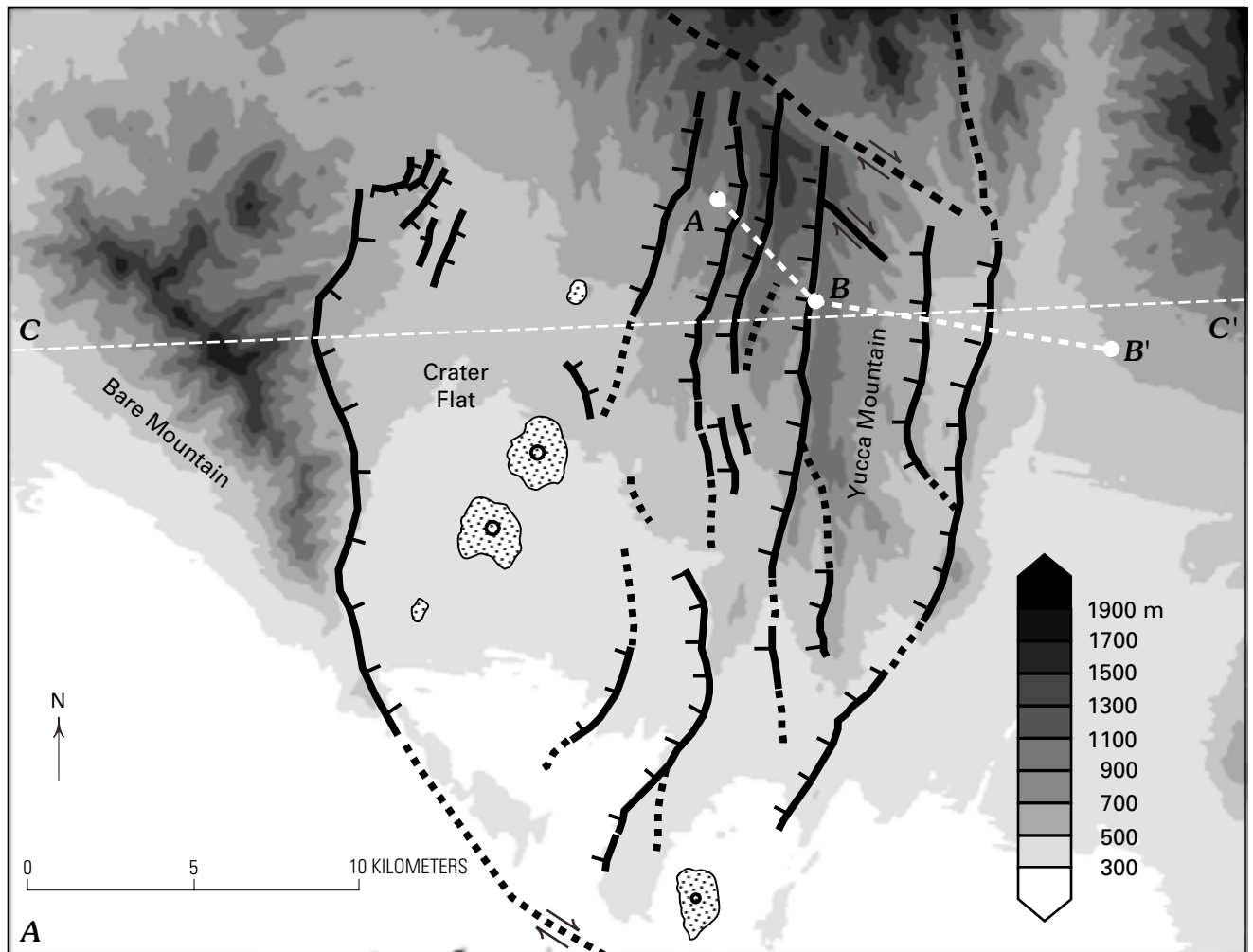
Cross-Sectional Models of Normal Fault Structures

Figure 1A shows the topography and faulting around Yucca Mountain, and figure 1B shows an interpreted cross section for Yucca Mountain, from Scott (1990). The cross section, like many normal faulting models, is based on the supposition that a major mechanical role is played by a detachment surface at depths of a few kilometers. An attempt to model the features hypothesized by Scott has been made by Young and others (1993); an example of such a model is shown in figure 2A. This modeling technique, widely used by structural geologists, assumes that simple shear collapse closes voids that would otherwise be created by slip on curved fault planes. The most basic elements of this balanced cross-section technique when applied to normal faulting are shown in figure 2B for a single listric fault. The model assumes, following Suppe (1985), that shear in the hanging wall is accommodated solely on a very large number of horizontal slip planes. This is not the only way of accommodating shear. Other interpretations assume, for example, vertical planes of multiple antithetic faults (as in Lucchitta and Suneson, 1993).

All listric fault models share certain features. First, the tilt of the beds in the hanging wall is determined only by the geometry of the curved fault, its slip distribution, and, in a minor way, by assumptions about shear processes in the hanging wall block. Second, the footwall block of a fault is completely undeformed and unrotated unless it lies in the hanging wall of another fault. In the field, however, footwall rotations are commonly observed when no suitable fault is present to explain them.

A serious problem for balanced cross-section models of normal faulting arises from observations of deformation associated with earthquakes. In general, geodetic observations before and after earthquakes, which determine the coseismic deformation, are well explained by simple isotropic elastic models, as emphasized by recent satellite radar observations of the Landers earthquake by Massonet and others (1993). Although an anisotropic element may be introduced by interseismic deformation, no evidence for this mechanism has been reported. Thus, the assumptions required to produce listric fault models do not seem to be consistent with observed earthquake behavior.

A model to explain geologic structures that is consistent with the observed behavior of earthquakes was introduced by King and others (1988) and Stein and others (1988). This model assumes that the upper seismogenic zone of the crust, nominally 15 km thick, together with the lower part of the crust, reacts in an elastic fashion at the time of an earthquake. Between earthquakes the lower crust relaxes stress by creep. The model incorporates isostatic compensation, which was also shown to be important by Wernicke and Axen (1988). Incomplete relaxation also occurs in the seismogenic zone such that its long-term elastic modulus is substantially lower than that determined in the short term. This reduction of modulus is conveniently described by assigning to the seismogenic layer an “effective elastic thickness” lower than its true thickness.



EXPLANATION

- Normal fault**—Dashed where inferred; teeth on downthrown side
- Strike-slip fault**—Dashed where inferred; barbs show sense of movement
- Basalt cone**
- C - - - - C'** Line of cross section

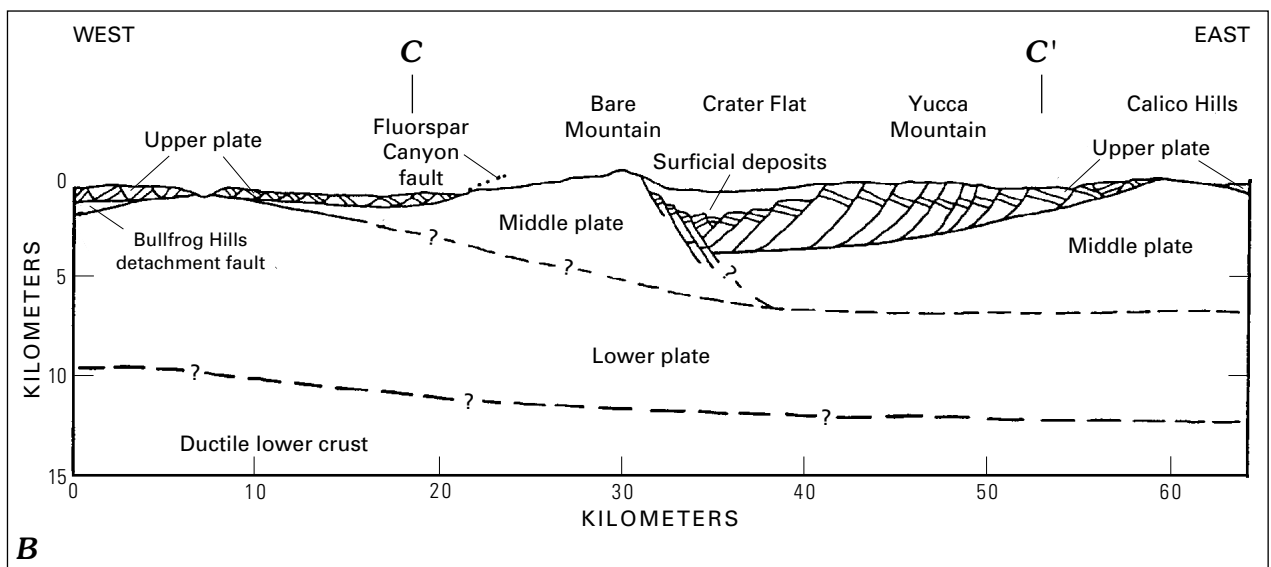


Figure 1. Relief map and cross section of Yucca Mountain area. *A*, Relief based on Digital Elevation Model from U.S. Geological Survey. Major faults are shown. *B*, Cross section assumes a detachment fault (queried) at depth (from Scott, 1990). Approximate line of profile C-C' is shown in *A*. Cross section A-B-B' shown in figure 2.

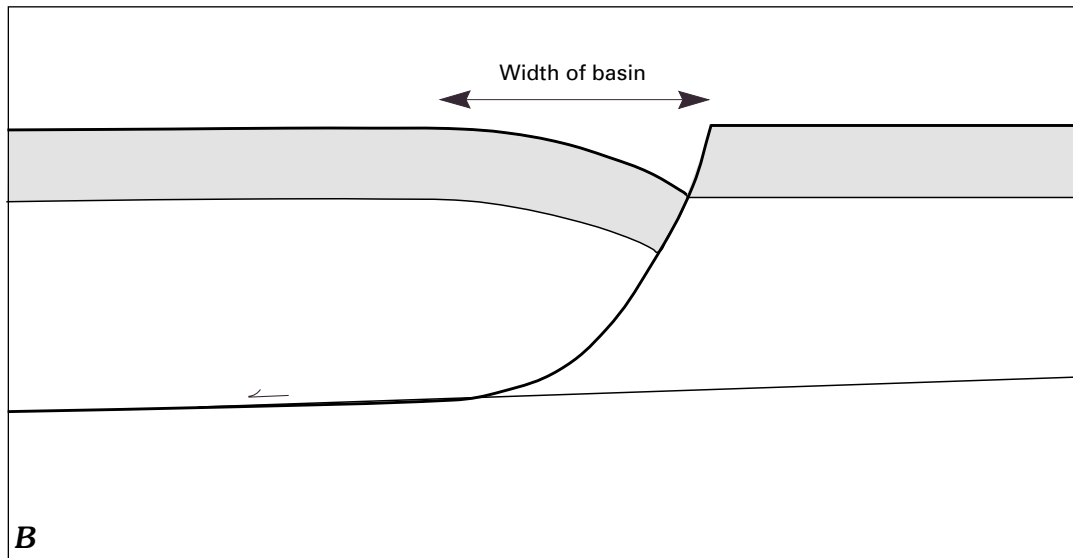
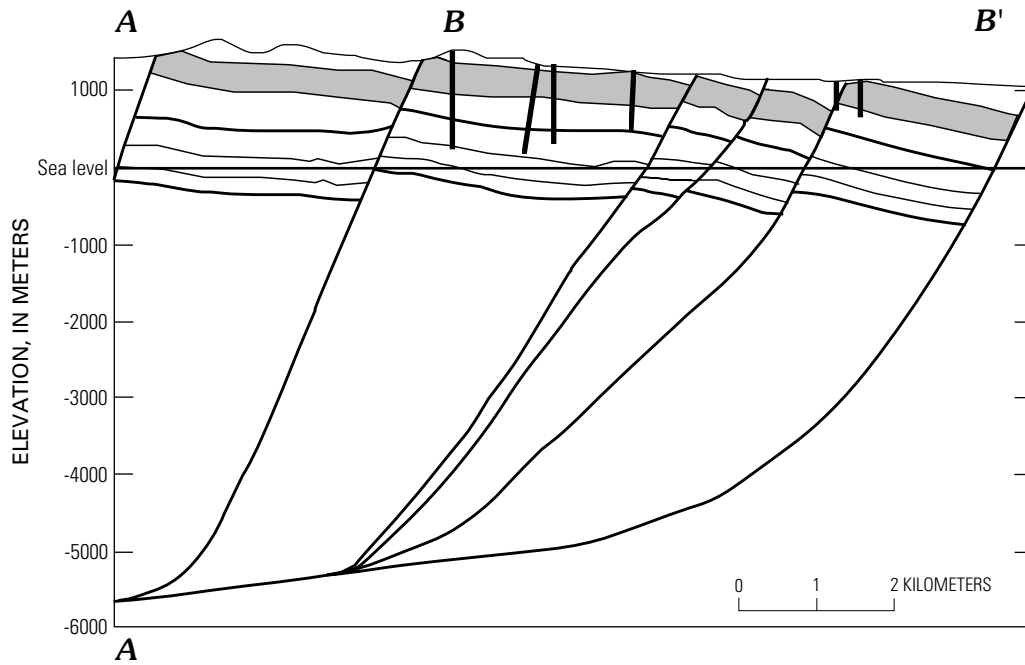


Figure 2. Modeled cross section of Yucca Mountain (*A*), and basic elements of balanced cross-section technique (*B*). *A*, Modeled cross section assumes simple shear on listric faults and a detachment fault at depth (modified from Young and others, 1993); line of section shown in figure 1*A*, and short near-vertical lines are boreholes. *B*, Prediction of the deformation of an idealized listric normal fault using rigid footwall assumptions consistent with Suppe style models (Suppe, 1985). Barb shows sense of movement.

Various authors have found values between 2 and 5 km; 2 km is appropriate for Basin and Range structures (Stein and others, 1988; Ellis and King, 1991).

To illustrate a simple application of our modeling methods, we apply data from the Virgin Mountains fault system situated on the Nevada-Arizona border (fig. 3). The results here presented are modified from King and Ellis (1990) and Ellis and King (1991). Geologic observations of the Virgin Mountains area show a wide, down-tilted sedimentary basin to the west, bounded by a normal fault with a throw of 15 km dipping to the west (fig. 4*A*). The Virgin Mountains themselves comprise an uplifted basement block thought, on petrological grounds, to

have risen more than 8 km. The estimated deformation of the original basement is shown in figure 4*B*. The uplifted block is apparently bounded on the east by a nearly vertical fault. Whatever the exact nature of this east-bounding fault, its association with surface folding clearly demonstrates contraction. Volcanoes occur in this region of contraction, an apparent anomaly inasmuch as volcanoes are thought to be associated with extension. The features just described seem to have been active simultaneously. This conclusion poses a problem for the usual explanations of structural geology. In particular, the simultaneous activity of extensional and contractional features is difficult to understand.

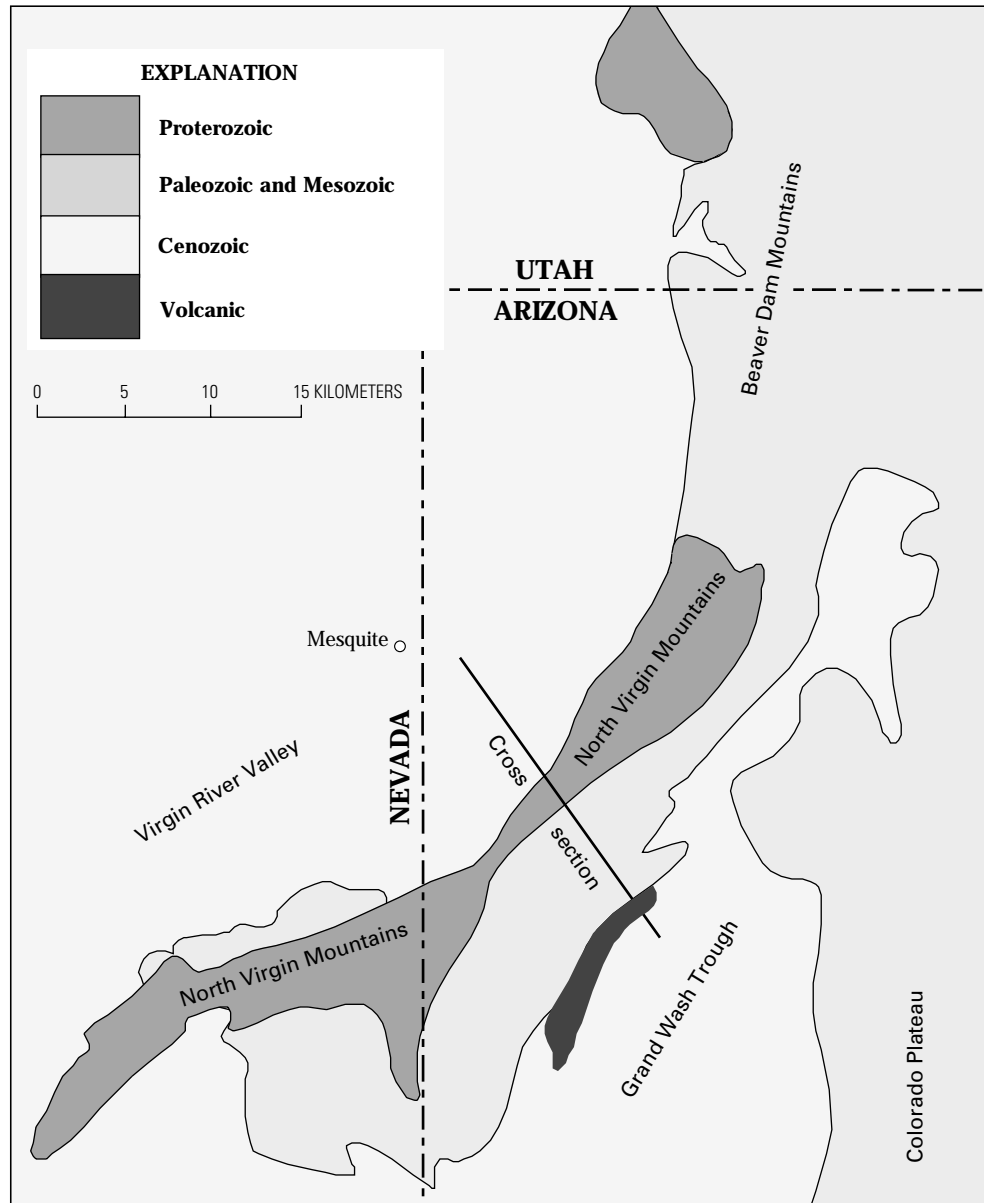
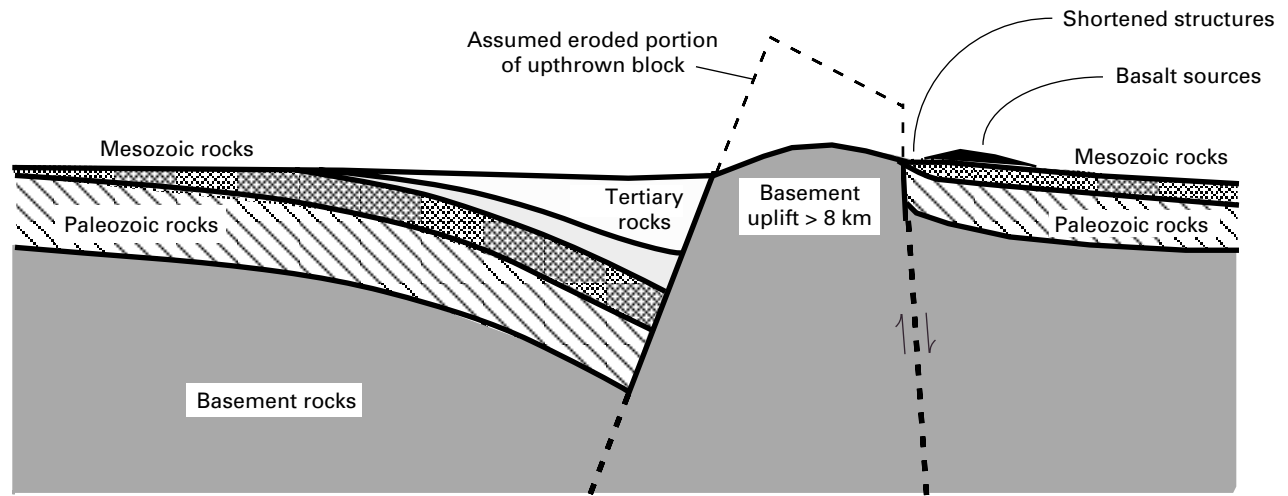


Figure 3. Simplified geologic map showing location of Virgin Mountains cross section in figure 4. (Modified from Wernicke and Axen, 1988.)

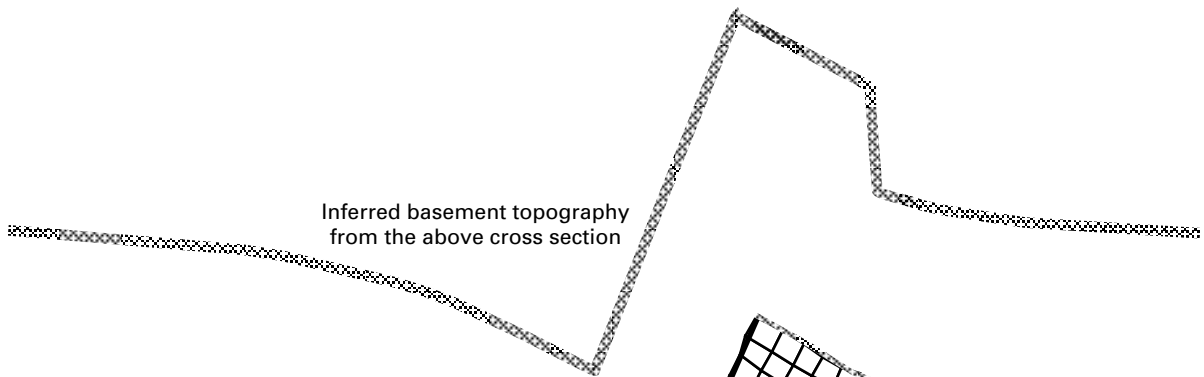
The model shown in figure 4C is calculated using a boundary-element method that is based on Crouch and Starfield (1983); see also King and Ellis (1990), Ellis and King (1991), and Gomberg (1991). It assumes a seismogenic crustal thickness of 12 km (Smith and Bruhn, 1984) with an effective elastic thickness of 2 km. A value for the density of the ductile lower crust of $2,900 \text{ kg/m}^3$ is assumed and the density of the seismogenic crust is taken to be $2,700 \text{ kg/m}^3$. At the surface, loads are applied to allow for the effect of erosion and deposition of sediment. To calculate these loads the sediments are assumed to have a density of $2,200 \text{ kg/m}^3$ and 80 percent of the uplifted Virgin Mountain block is assumed to have been removed by erosion.

The mechanical processes involved in the model can be understood by considering that the uplift of the central Virgin Mountains block is driven by the buoyancy of the root zone

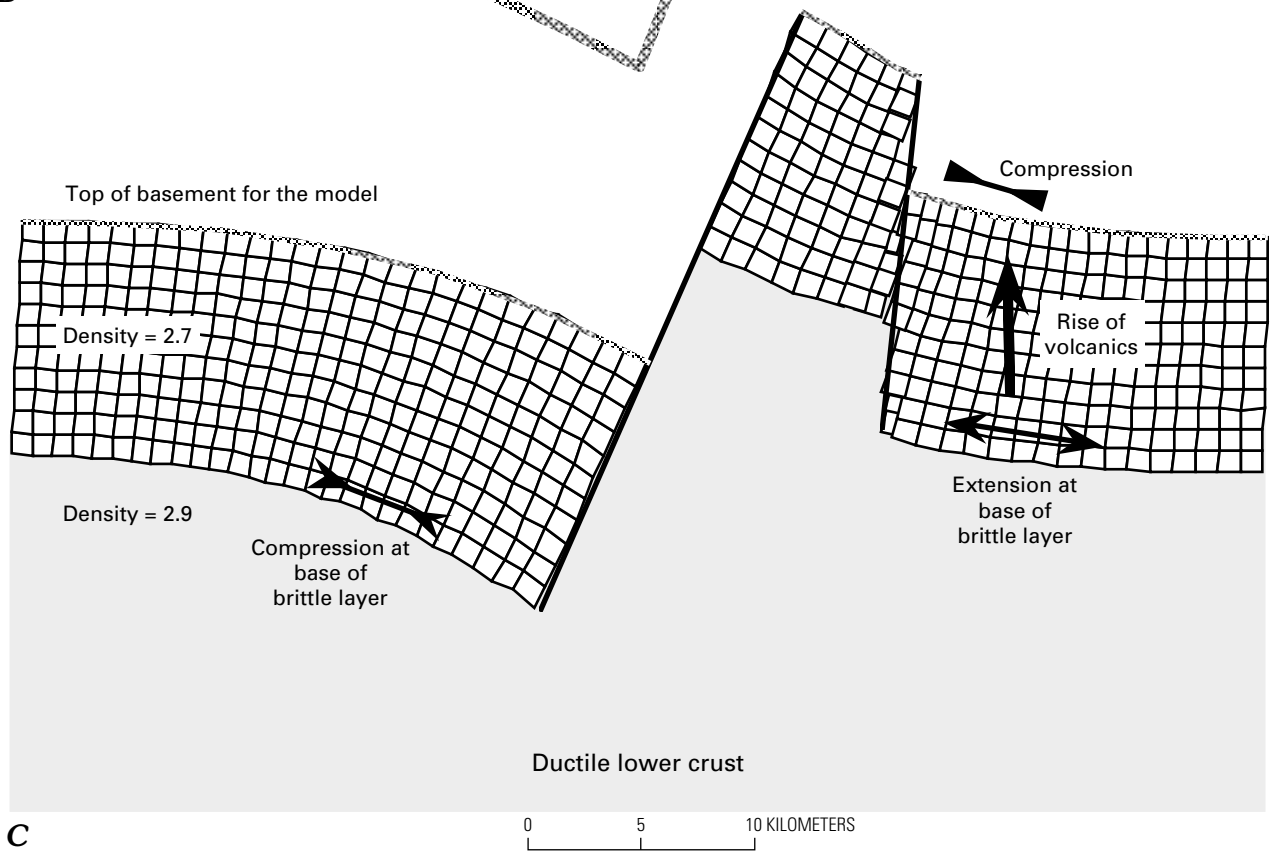
beneath. Subsidence of the hanging walls results from the lack of buoyant roots. Because the crust does not behave in a rigid fashion, the hanging walls in the vicinity of the central uplifted block will warp under the applied load as shown in figure 4C. The downward flexure of the basin in the west can now be seen to be a result of a combination of buoyancy effects and warping under sediment load. The observed features are not the result of a listric fault at depth, which is the only way in which balanced cross-section models that assume a rigid footwall can explain such features. Buoyancy, and not horizontal forces, drives the uplift of the Virgin Mountains, and the uplift is accommodated by slip on the vertical fault on the range's east side. Flexure gives rise to other effects. The lower part of the footwall block is extended, and the upper part is in compression. Ellis and King (1991) argued that the location of volcanism is controlled by stress conditions at the base of the brittle crust, which,



A



B



C

Figure 4. Schematic cross section of Virgin Mountains, and applications of model. *A*, Section, from King and Ellis (1990) and Ellis and King (1991). Faults at depth dashed where inferred. *B*, Inferred basement topography. *C*, Deformation model.

because of flexure, is extensional below the volcanic edifices. Once magma starts to rise, hydraulic forces allow it to continue to produce the apparent anomaly of volcanoes appearing amid compressional features.

The model explains a range of observations in a simple way. Flexure and buoyancy are important elements that are rarely included in geological models. The model also invokes a rheological model that is consistent with contemporary concepts of earthquake mechanisms, including the global lack of observation of focal mechanisms consistent with listric normal faulting and the observation that all major events in extensional regions are on planar faults dipping between 30° and 60° which completely traverse the seismogenic zone (Jackson, 1987).

Two-Dimensional Modeling of Dip-Slip Planar Faults Incorporating Buoyancy and Erosion and Deposition of Sediment

Using modeling techniques that include the effects of buoyancy and the erosion and deposition of sediment, King and Ellis (1990) and Ellis and King (1991) determined the maximum possible fault throws that could result from buoyancy forces. The fault systems were freely moving and permitted to slip until an equilibrium between gravitational and flexural forces in the plate was reached. Calculating maximum possible displacements for Yucca Mountain is not a concern. Thus, fault slip may be specified rather than stress conditions, allowing models to be calculated more rapidly. Final models with the same fault slip are identical with models where the fault slip has resulted from adjusting stress conditions, and only buoyancy forces determine the form of the final deformation.

The effects of different parameters on the deformation have been investigated. Figure 5 summarizes the results relating to a simple, single fault with a throw of 5 km, cutting a 12-km-thick elastic layer. The layer is assumed to have a reduced rigidity such that its effective elastic thickness is 2 km. Although not shown in figure 5, the deformation is calculated as if erosion cuts material from the footwall and sediments fill in the void over the hanging wall. This redistribution of loads changes the shape of the structure. In figure 5A, the section labeled 30 percent is for the case in which 30 percent of the uplifted material is cut away and the subsidence is filled by a mass of material equal to 30 percent of material that previously filled the new void. The same interpretations apply to the section labeled 60 percent. The effect is substantial only when the amount of erosion and sedimentation surpasses 60 percent (depending on the effective elastic thickness).

Figure 5B shows the effect of changing the effective elastic thickness from 2 to 8 km while keeping fault throw (5 km) and erosion and deposition of sediment (30 percent) constant. Width of the structure and tilts of hanging wall and footwall are very sensitive to changes of effective elastic thickness, because the width of structures is related to the degree of flexural bending and that in turn is sensitive to effective elastic thickness.

Figure 5C shows the effect of changing fault slip for a constant elastic thickness (2 km) and erosion and deposition of

sediment (30 percent). Hanging wall and footwall dips are proportional to fault slip.

Yucca Mountain is cut by many faults; thus, the effects of faults interacting must be considered. Figure 5D shows the effect of five faults each with a throw of 1 km. From this and other tests not shown here, it appears that changes in dip or faults joining at depth do not change surface features in an important way.

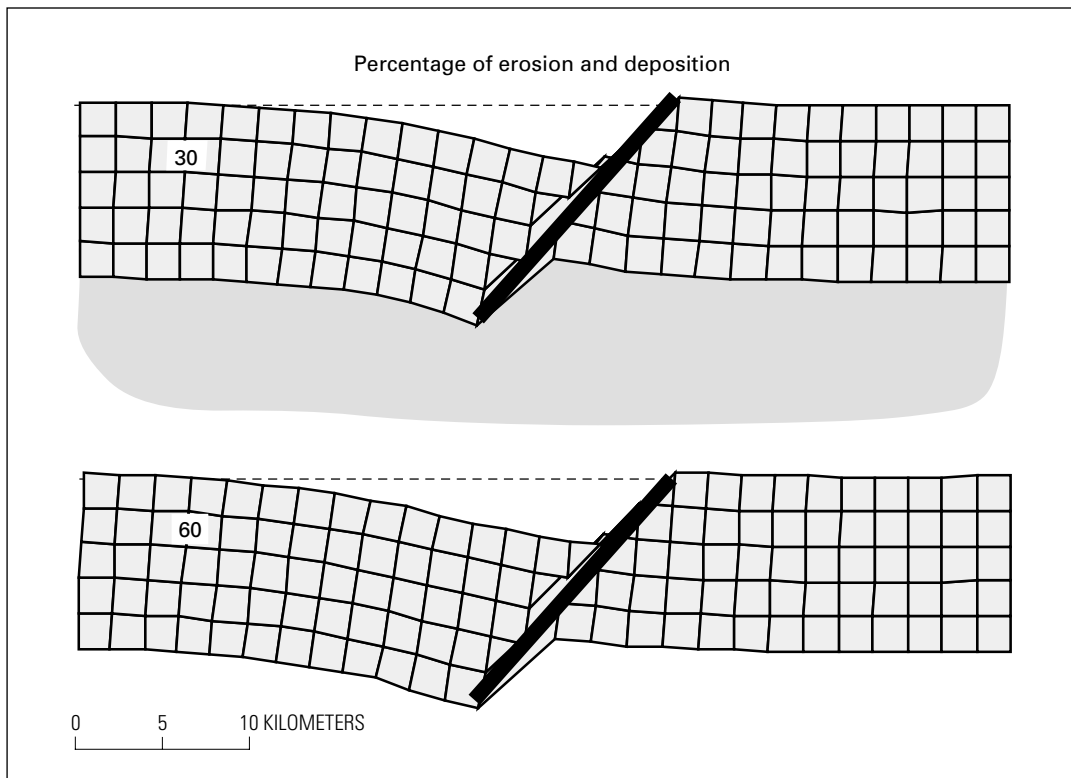
Note that the multiple faults in figure 5D result in “necking” of the brittle crust that gives rise to subsidence. Some difficulties associated with Yucca Mountain modeling can be understood from this. Faults are mapped both east and west of Yucca Mountain. Thus, if we regard Yucca Mountain as being one of the central blocks in figure 5D then it should be lower, rather than higher, than surrounding regions. The assumptions required to create models that do not make Yucca Mountain lower than surrounding features are discussed in the next section.

Figure 5A–D indicates that fault geometry at depth does not change surface features in an important way. Total fault slip and effective elastic thickness are much more important. Within the bounds likely to be appropriate for Yucca Mountain, changing sediment deposition and erosion, or average fault dips, can modify models only in a minor way.

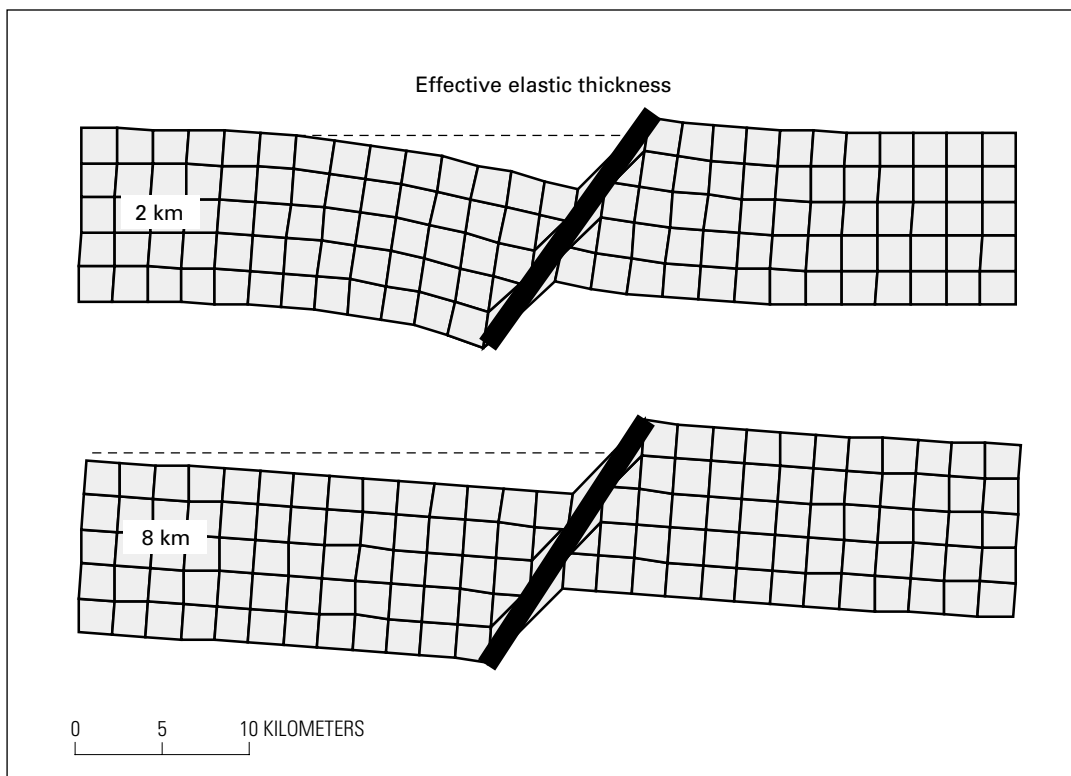
Two-Dimensional Yucca Mountain Models

The objective behind two-dimensional modeling was to create cross sections compatible with the observations on which figure 1B is based, but without assuming the same processes at depth. The reasoning behind the creation of a satisfactory model is summarized in figure 6. The seismogenic zone is 12 km thick. Faults dip at 75°. For the reasons explained earlier, only large changes of dip alter the models substantially, and it is not important whether or not faults join at depth. All the models shown use an effective elastic thickness of 2 km and assume erosion and deposition of 30 percent. The latter is probably excessive for Yucca Mountain and underestimates the sediment load in Crater Flat, but, as previously stated, the errors involved are small.

Figure 6A shows the geometry of the region modeled. In figure 6B–E only the gridded region of figure 6A is shown with vertical exaggerations of 2. The regions with shaded lines are included in these figures only to show how boundary conditions have been applied and affect the final model; these conditions are not required to fit the observations. Faults are identified in figure 6B; the Windy Wash and Fatigue Wash faults are shown as one and a fault we refer to as the Crater Flat fault is introduced beneath Crater Flat. In addition, figure 6B includes two boundary condition faults, whose role is discussed in the next paragraph. Figure 6C shows the deformation due to motion on all faults except the Crater Flat fault and the boundary condition faults. Slip values are taken from Scott (1990). Neither Bare Mountain nor Yucca Mountain is sufficiently uplifted in relation to other features for this model. In figure 6D, motion is introduced on the Crater Flat fault, but even this will not produce the required uplift of Yucca Mountain.

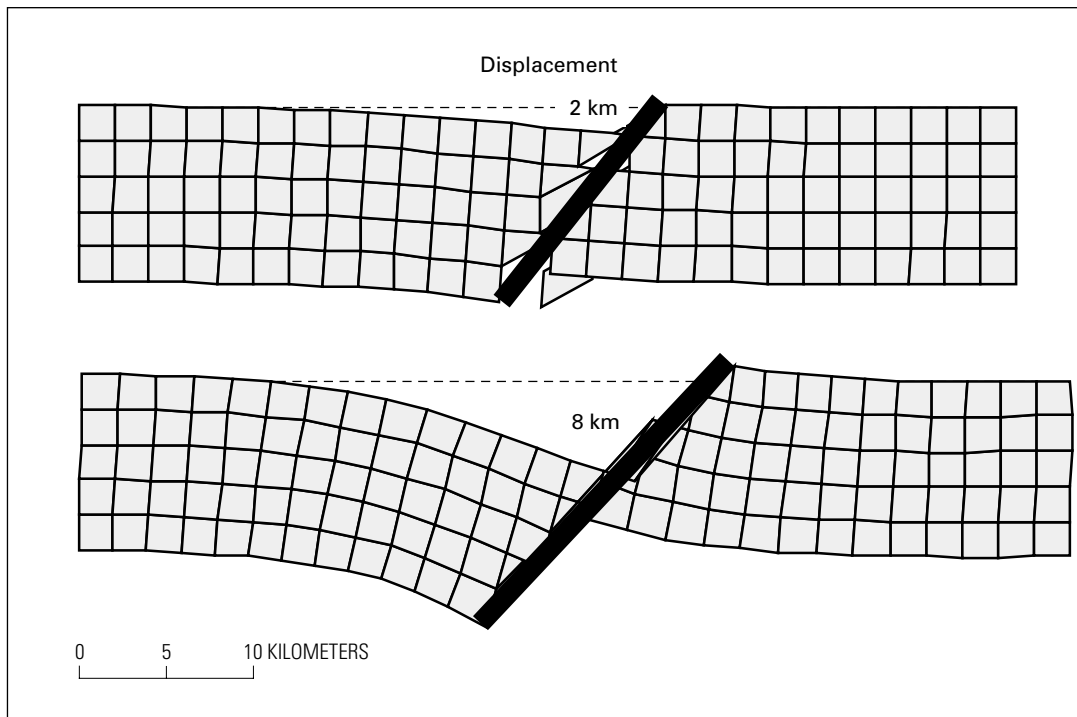


A

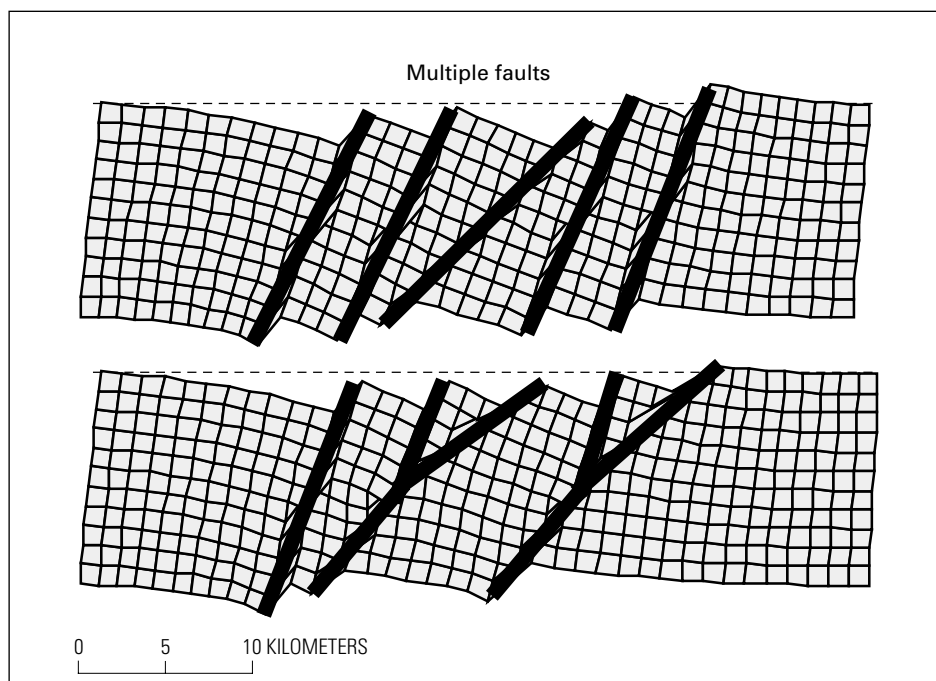


B

Figure 5 (above and following page). Effects of changing model parameters. *A*, Effects of changing proportion of erosion and deposition of sediment. Grid is at 2 km intervals and only the interval from 1 to 11 km is plotted. Dashed line, undeformed surface. *B*, Effect of changing effective elastic thickness while keeping fault slip (5 km) and erosion and deposition of sediment (30 percent) constant. *C*, Effect of changing fault slip while keeping erosion and deposition of sediment (30 percent) and effective elastic thickness (2 km) constant. *D*, Effects of changing fault dips and allowing faults to join at depth.



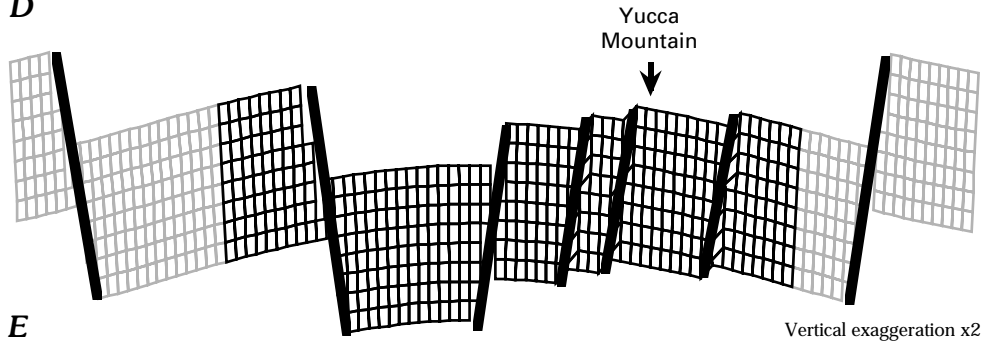
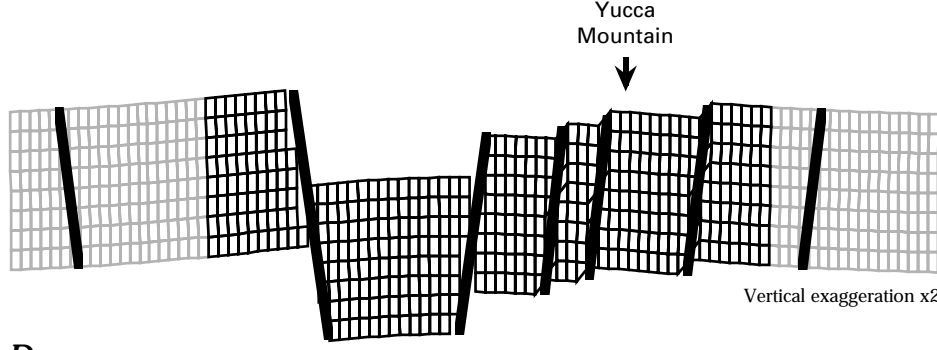
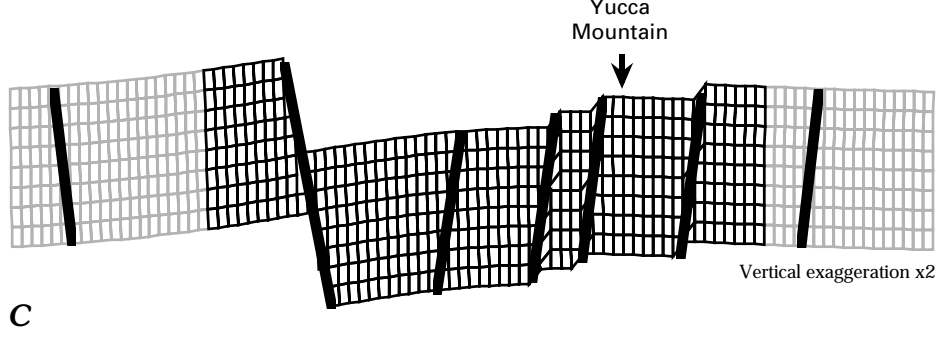
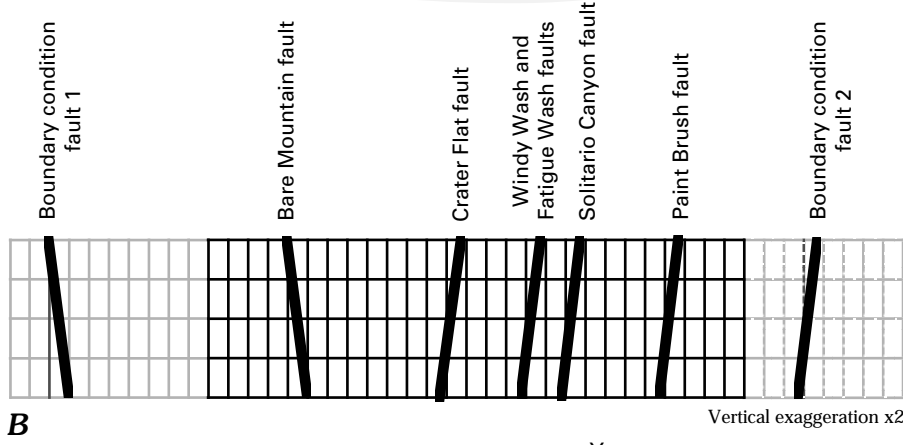
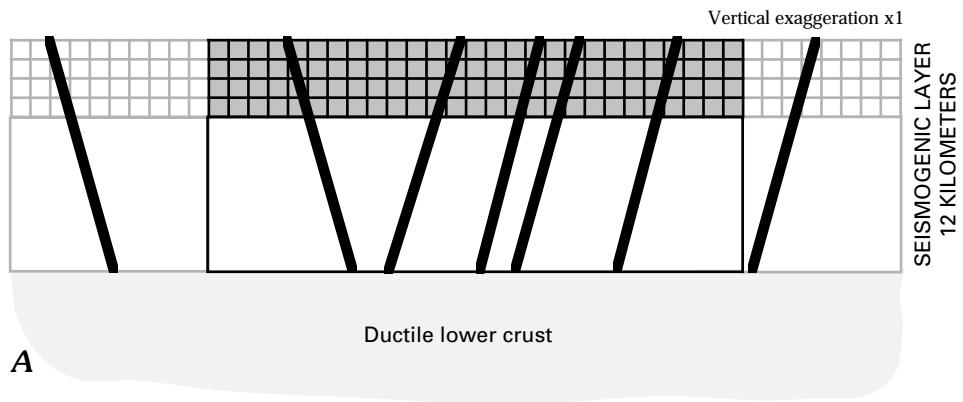
C



D

The presence of normal faulting implies extension and necking of the crust. Necking of the crust is linked with flexure at the flanks and isostatic subsidence of the stretched crust, causing topography to be too low in the center of the model, as if it were situated in a basin. This scenario is obviously not correct since extension of the crust is not localized around Yucca Mountain only. The two boundary condition faults correct for this. The throw on these normal faults is such that regional crustal subsidence is produced that is

comparable to that in the (nonshaded) zone of interest. The overall average isostatic subsidence is now equalized. The uplift of Bare Mountain and Yucca Mountain relative to their surroundings improves dramatically as shown in figure 6E. This does not imply that these faults exist, although a density of faulting giving overall stretching similar to that observed in Yucca Mountain is required. For further discussion, see the section, "A Model for Yucca Mountain Based on Observed Displacement."



Results from Planar Dip-Slip Modeling

Conclusions of the foregoing two-dimensional modeling are as follows:

- Models which incorporate buoyancy effects can explain bedding dips as a result of slip on planar faults.
- The existence of a detachment surface is not required to explain the surface observations.
- Bedding dips in rotated fault blocks depend upon the effective elastic thickness and cumulative vertical throw.
- Bedding dips do not depend much on fault dips. If faults of different dips intersect at depth they behave in the same way as planar ones that do not intersect.
- A satisfactory Yucca Mountain model using existing slip estimates can be produced provided that (1) some slip has occurred on a west-dipping fault or faults beneath Crater Flat and (2) subsidence similar to that resulting from faulting associated with Yucca Mountain has occurred outside the Yucca Mountain region. This subsidence is probably due to unidentified faulting. In the absence of such faulting, it might be necessary either to propose uplift of Yucca Mountain by magmatic processes in the crust, or to attribute an important role to preexisting topography.

Shear-Zone Modeling in Plan View

That strike-slip deformation plays an important part in Basin and Range deformation has become increasingly clear over the last 10–15 years (Hill, 1982; Ron and others, 1986). In particular, strike-slip components on Yucca Mountain faults are important and may even be dominant. Various descriptive models that may be applied to Yucca Mountain have been proposed; they have attracted names such as “bookshelf” or “rotating beam” faulting (McKenzie and Jackson, 1986; Nur and others, 1986). Figure 7 shows a system in which a series of parallel beams are terminated by pivots. These pivots fall on two parallel lines that may be regarded as bounding the shear zone. The lower line is fixed; the upper line is translated by the overall slip vector D that is applied to the zone. A direct geometric relation exists between the slip vector and the strike of the internal faulting; the vector must be perpendicular to the strike of the faults separating the blocks or internal deformation of the blocks will occur. If the dips of the faults are known, the strike-slip and dip-slip components of motion relate in a simple way to the strike of the shear zone and the length and width of fault blocks. The configuration of figure 7 will show dilation and strike-slip on faults.

Figure 6 (previous page). Two-dimensional modeling of Yucca Mountain. Line of cross sections approximates $C - C'$ in figure 1A. For further information about modeling method, see King and Ellis (1990). A, Relation of faults to the 12-km elastic layer. Only the gridded region is reproduced in views B–E. B, Gridded region is shown at a vertical exaggeration of 2, and faults are identified. Rectangles measure 2×2 km. C–E, Deformation is shown for different combinations of fault movement (see text). Each rectangle measures 1×1 km.

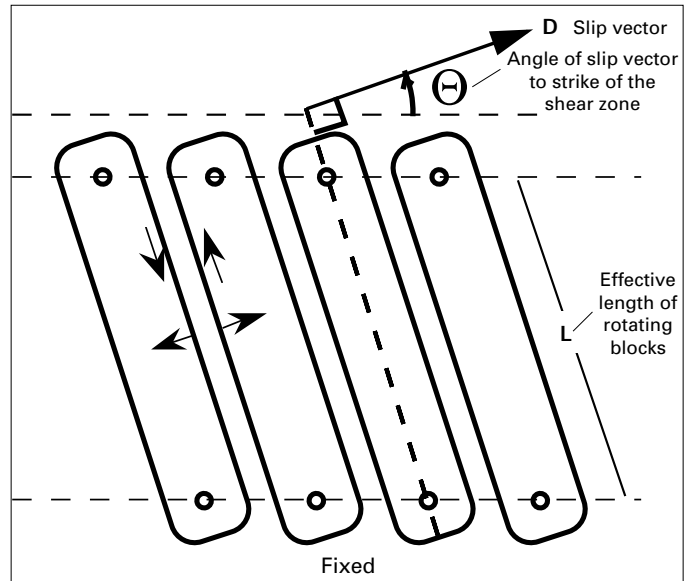


Figure 7. Geometric relations for a shear zone composed of rotating blocks.

Boundary Conditions and Models of Yucca Mountain

Figure 8A shows a map of the faulting around Yucca Mountain. A first approach to modeling this system using a series of simple faults (fig. 8B) is directly comparable to the block models discussed previously (fig. 7). Figure 8C shows a typical two-dimensional deformation field, driven by displacement on two distant boundaries.

For the faults in the center of figure 8C, the overall ratio of strike-slip to opening is similar to that predicted for block models. For the models, however, the slip tapers at each end of the faults, and complicated strains occur at the ends (where the pivots are found in the simple beam models). These strains include shear, extension, and compression. The faults at the ends of the zone have a much larger opening displacement and smaller shear slip than those at the center and are very different from the block model prediction.

Unlike the system of faults depicted in figure 8B, Yucca Mountain is not isolated in an otherwise uniformly deforming medium; thus the model shown in figure 8B is unrealistic. Producing a realistic model requires that the fault kinematics be known for some distance outside the region. In other words, we must add more faults than those we wish to model in order that the region of interest behaves correctly. This same requirement was encountered in two-dimensional cross-sectional modeling. If extra faults, similar to those already shown, are thus added to the left and right, peak normal and shear slips become similar to those predicted for an equivalent block model. Again, much deformation occurs near the pivot regions where complex deformation is to be expected.

Evidence does exist that shear may enter the Yucca Mountain region along narrow zones rather than being imposed on more or less distant boundaries. Figure 8A shows suspected or inferred northwest-southeast-striking strike-slip faults to both

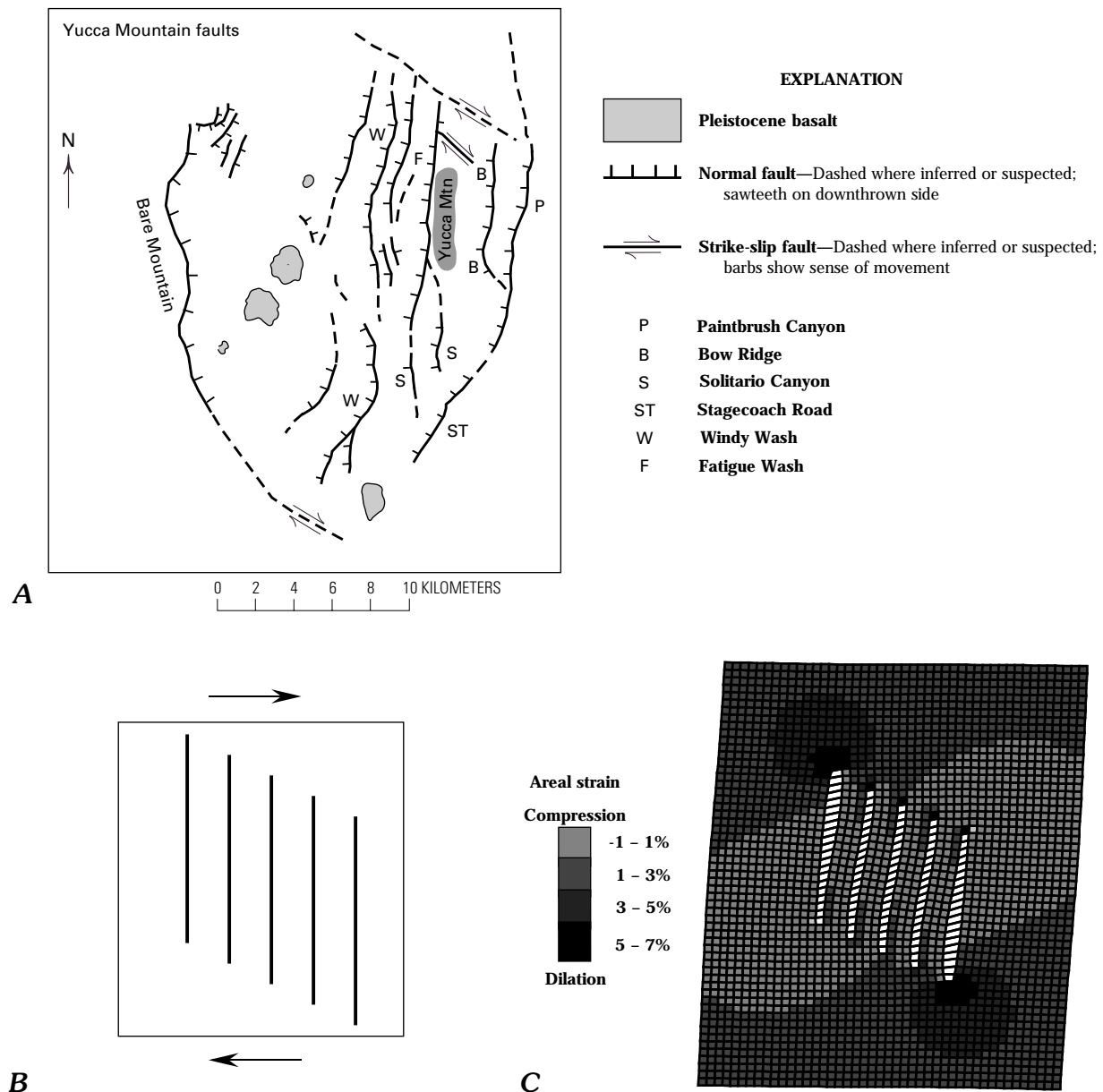


Figure 8. Faults and fault models, Yucca Mountain. *A*, Faults around Yucca Mountain (based on Silvio Pezzopane, written commun., 1994; Frizzell and Shulters, 1990; Scott and Bonk, 1984; Scott, 1990, and O'Neill and others, 1992). The fault inferred to be buried underneath Crater Flat is not shown. *B*, A simple block-faulting scheme used to explore relations between boundary conditions and fault-slip style. *C*, Modeled deformation under imposed regional shear.

the north and the south of the Yucca Mountain system. Should such features extend farther to the northwest and to the southeast, respectively, the Yucca Mountain region could be viewed as an extensional zone lying within this offset. This mechanism has been proposed previously for faults in the Las Vegas shear zone (Liggett and Childs, 1974) and is shown in a simplified form in the model in figure 9*B*. The left-hand north-south-striking fault, equivalent to the Bare Mountain fault, has predominantly normal motion decreasing from north to south. The central two faults, equivalent to Windy Wash, Solitario Canyon, and so forth, have combined normal and strike-slip motion. However, this slip does not decrease in amplitude from north to south.

The oroclinal bending that is observed in the field with rotations increasing from north to south (Nelson and Jones, 1987; Rosenbaum and others, 1991), cannot be modeled in this way. However, a slightly more complex model which incorporates elements of figures 8*C* and 9*A* can produce this effect. Small faults are also introduced at the south ends of the blocks as shown in figure 9*B* such that rotation occurs as if pivots were put in place. Oroclinal bending now occurs (fig. 9*C*). In practice, such pivoting requires intense localized deformation near to the pivots; features around Lathrop Wells may be associated with such deformation.

The combined result of these boundary conditions is to produce a model that is kinematically similar to the Yucca

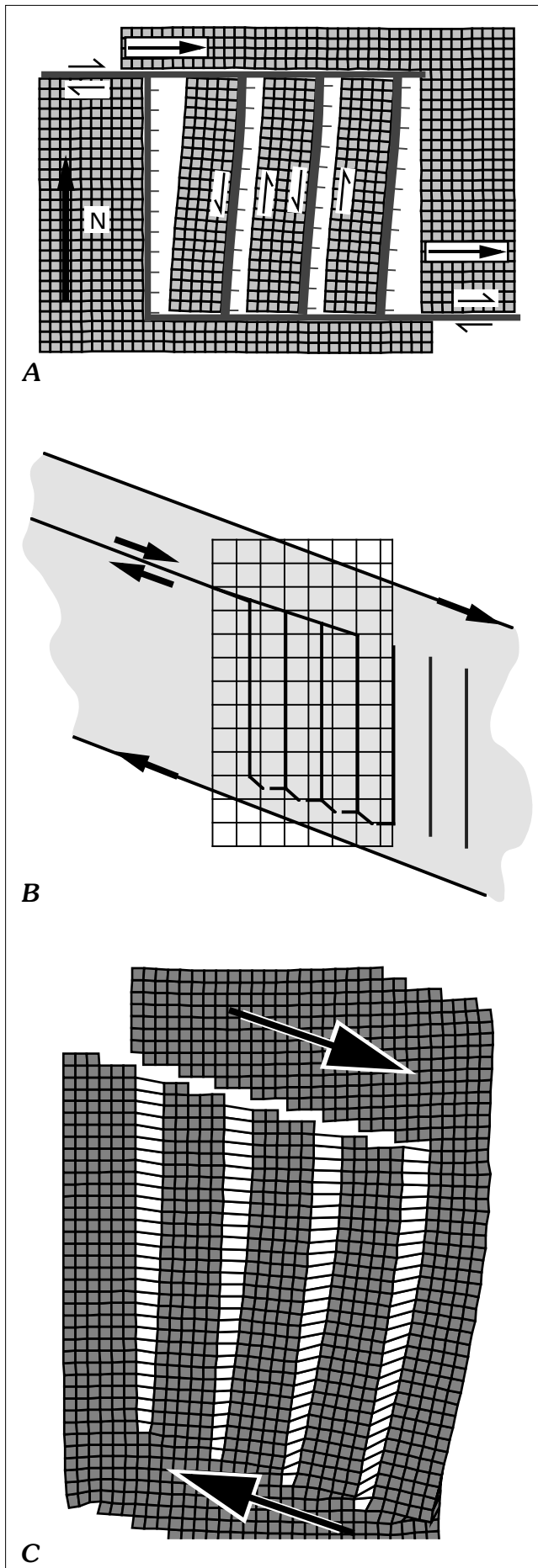


Figure 9. Three models showing effects of shear deformation on rotating blocks. *A*, Exploring conditions when shear enters region in a localized fashion (a system of rotating blocks accommodating a fault step-over). *B*, Incorporating distant boundary deformation, localized shear on upper left and more distributed shear on right. Rotation at lower pivot regions is made easy by addition of extra small faults. *C*, A model kinematically similar to Yucca Mountain.

Mountain system (fig. 9C). The leftmost fault is taken to be Bare Mountain and the other faults those of the Yucca Mountain system. In all cases slip diminishes to the south, although, in proportion, left-lateral slip is greatest to the south. These values can be adjusted with small changes in the boundary conditions.

The modeling suggests that the following may exist:

- A localized shear zone extending to the northwest of Bare Mountain, or some other structure that satisfies similar conditions at that edge of the model.
- A broad shear to the east probably consisting of roughly north south faults similar to those of the Yucca Mountain system.
- Intense complex deformation at the south end of the Yucca Mountain faults.

In the absence of better regional information, further refinement of the foregoing models directly seems unreasonable. Rather than use the boundary conditions to predict fault slips, we have fixed the slips for many Yucca Mountain faults from the available data to determine whether this produces a sensible model. This process sheds light on other aspects of the problem of establishing the boundary conditions needed to model Yucca Mountain.

A Model for Yucca Mountain Based on Observed Displacements

The simplified set of faults on which slip is fixed is shown in figure 10. The fault slips to be assigned to these faults are taken from Scott (1990). The Bare Mountain fault is assumed to dip 75° E., and the other faults are assumed to dip 75° W. The hypothesized Crater Flat fault is given the slip needed to reproduce a reasonable relative uplift of Bare Mountain and Yucca Mountain. This fault plays the same role in the three-dimensional as in the two-dimensional modeling. Without it, Yucca Mountain is too low. Two outer boundary condition faults are also included and again play the same role as in the two-dimensional modeling (these faults are shown with arrows, indicating that they are, in fact, longer). Erosion and deposition were taken to be 30 percent, which, like the two-dimensional model, probably overestimates erosion and underestimates deposition. Because of the variation of erosion and deposition along the strike of the features, using direct estimates of sediment loading and unloading would be more appropriate than exploiting the automatic procedure in the program. This would require more information than we have at present, but, as previously noted, major features of the model would not change if erosion and sedimentation were incorporated more carefully.

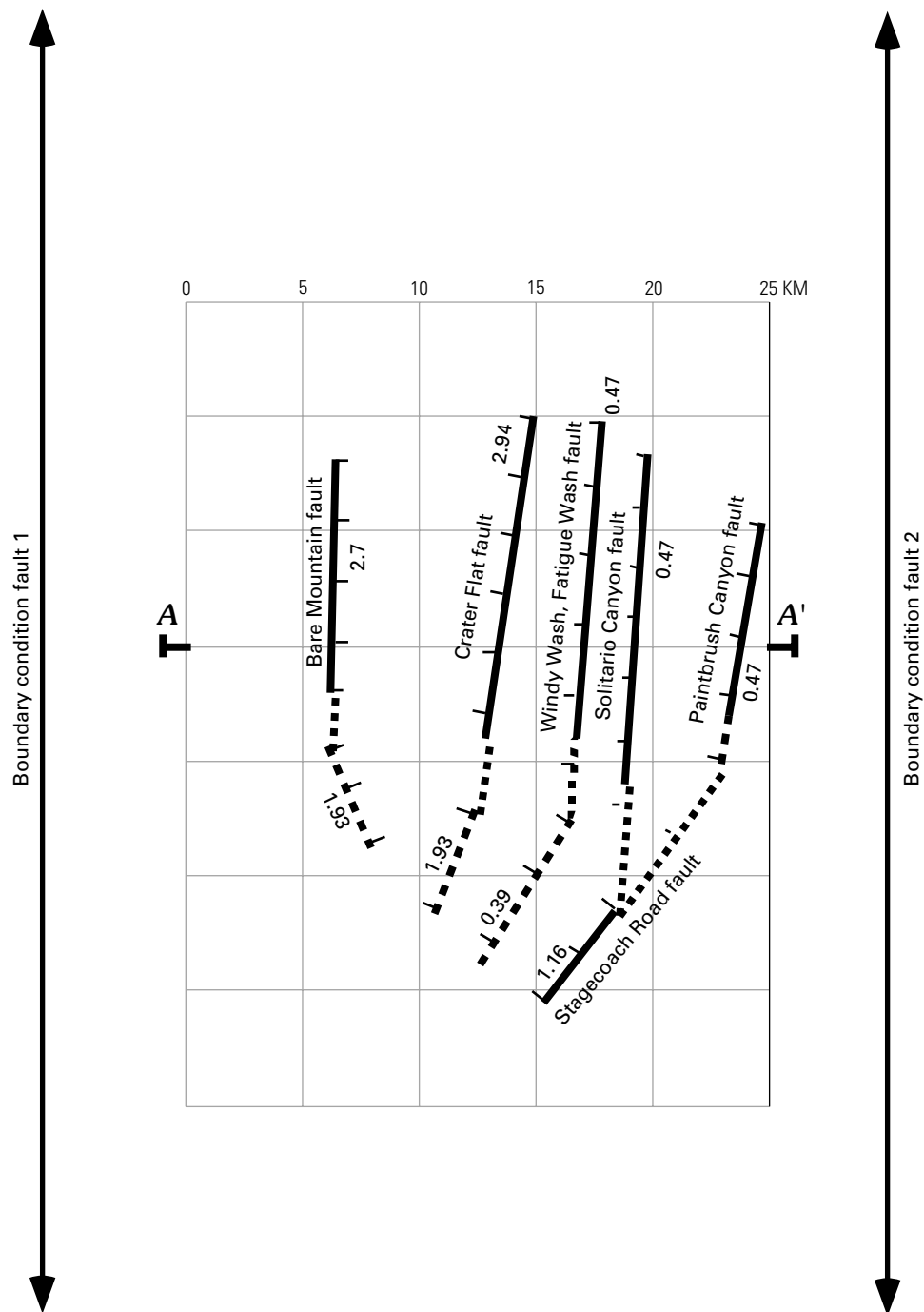


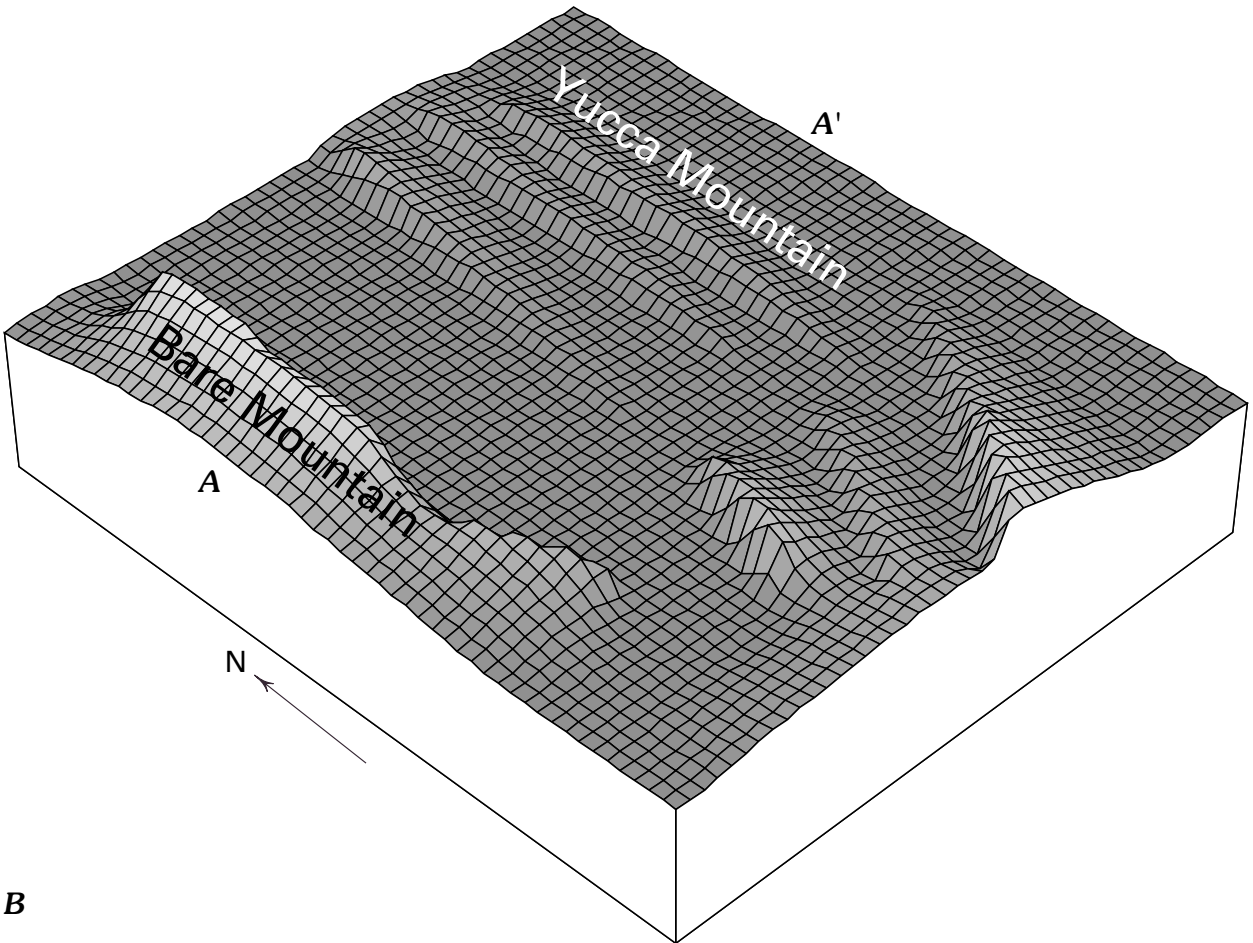
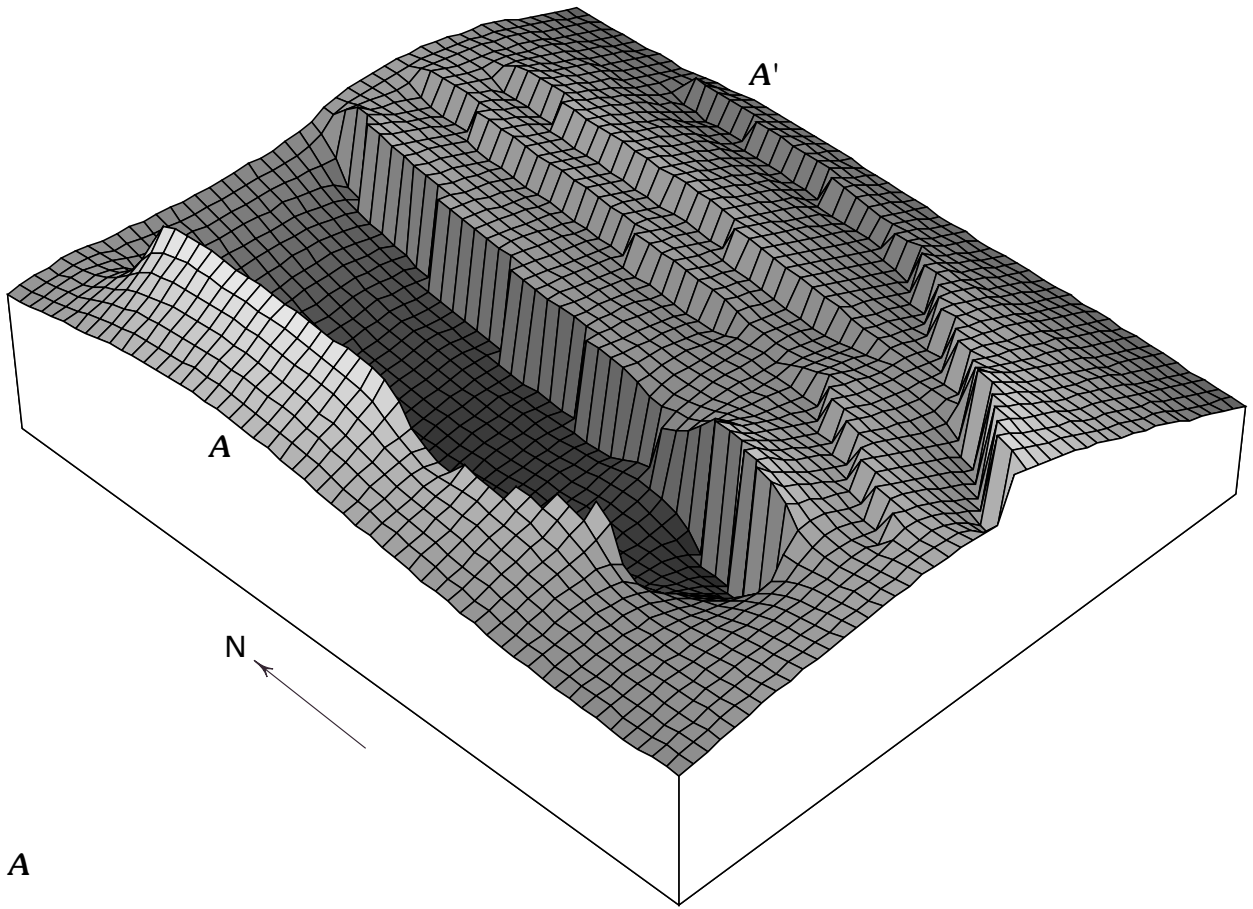
Figure 10. The simplified fault system used to generate a three-dimensional model for Yucca Mountain based on current estimates of fault throws. Numbers are throws (in kilometers) taken from Scott (1990); hachures on downthrown side; concealed or inferred fault segments are dashed. See figures 11 and 12 for cross section A-A'. Area shown in models is indicated by an arbitrary grid system (in kilometers).

Figure 11A shows the deformation for the system of faults shown in figure 10. The effective elastic thickness used is 2 km, and erosion and deposition of sediment are 30 percent each. The model captures the main features of Yucca Mountain and the surrounding faulted blocks.

The model shown in figure 11B is based on the one shown in figure 11A, but adjusted to fit observed topography. All points that lie below a plane that gently slopes from north to south have been set to the value of the plane at that point. This has the

effect of “filling” the valleys to approximate the presence of sediment. To reflect the effect of erosion, the model has been smoothed. This is an over-simplified approximation, but

Figure 11 (following page). Three-dimensional model showing deformation on faults at Yucca Mountain. A, Deformation due to slip on faults shown in figure 10. Vertical exaggeration $\times 3.5$. B, Low elevations in A have been filled with sediment and high elevations have been smoothed to represent effects of erosion.



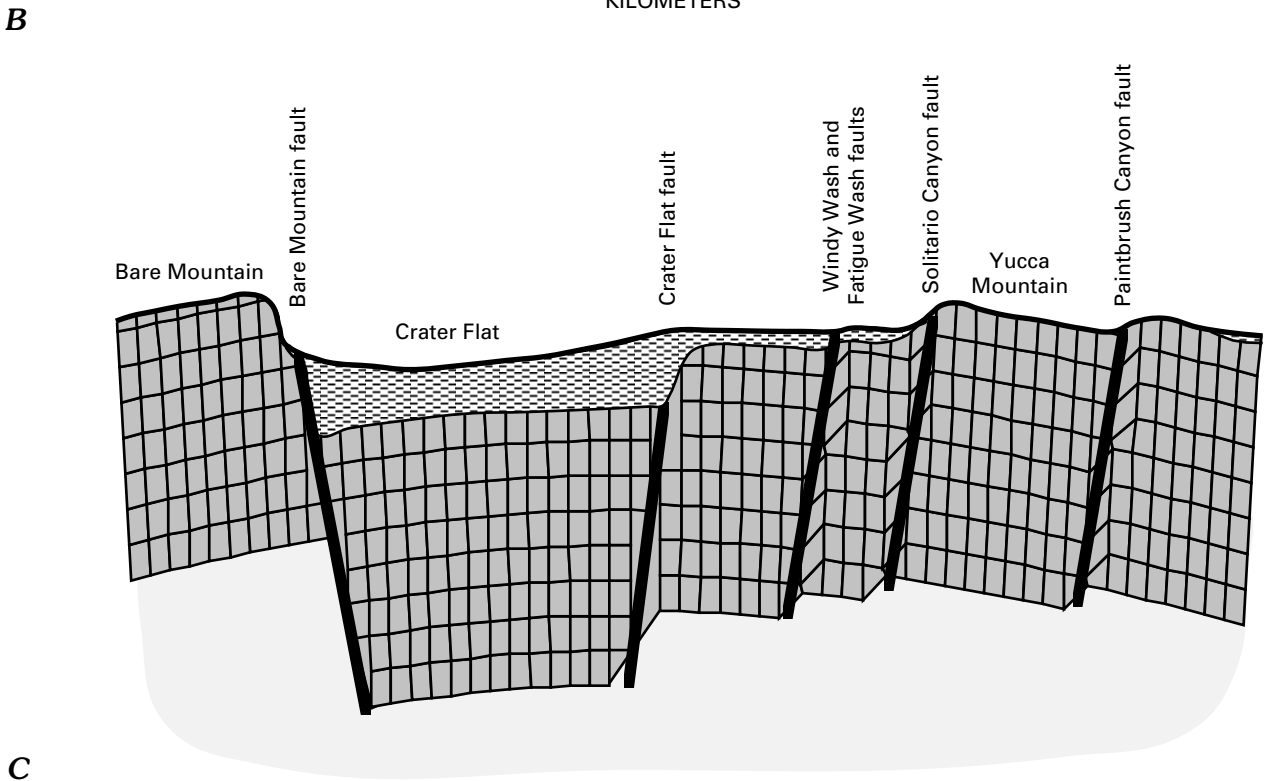
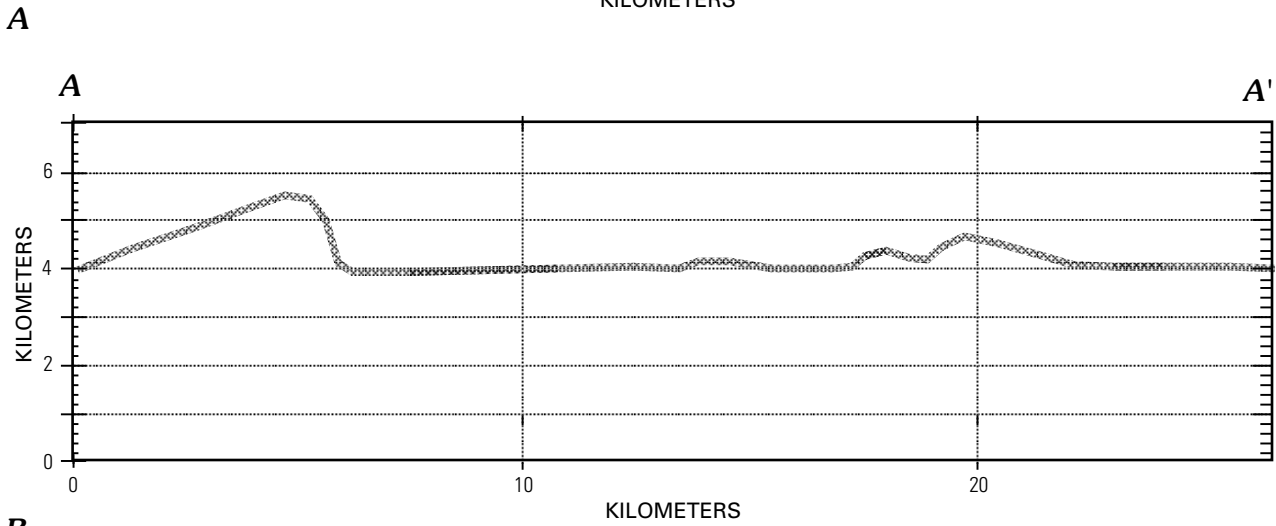
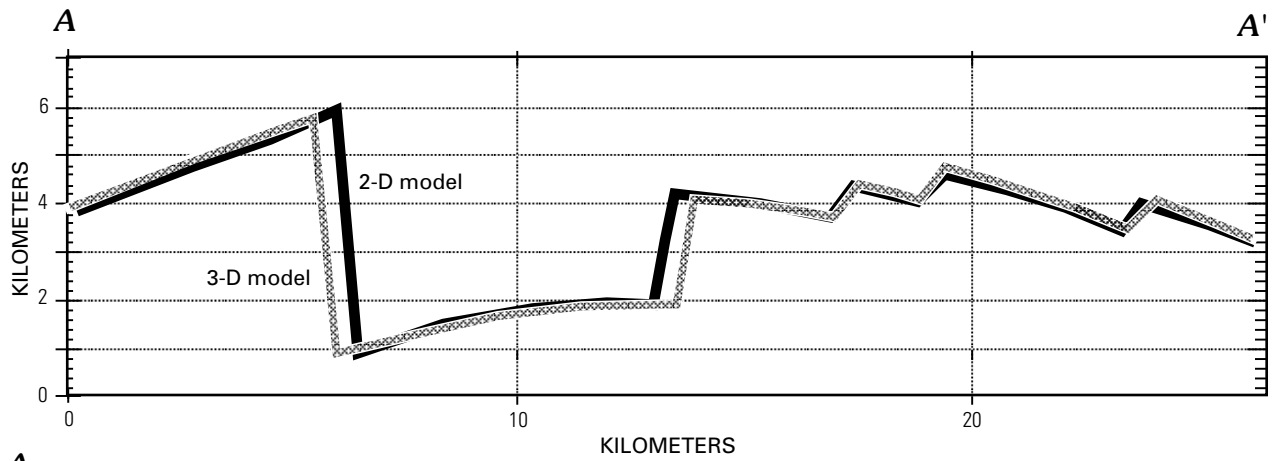


Figure 12. Yucca Mountain profiles and cross sections. *A*, Two-dimensional cross section shown in figure 6*E* and three-dimensional model of figure 11*B* to show the compatibility of the two methods. *B*, Profile A-A' along the smoothed three-dimensional model of figure 11*B*. *C*, Profile of topography taken from Scott (1990) along C-C' (see fig. 1*A*) added to cross section of figure 6*E* as described in text.

nonetheless, the overall match to the topography of the region is good. (Compare with figure 1A.)

Figure 12A shows a comparison between profiles computed using the two-dimensional cross-section assumptions and the three-dimensional plan-view model. Figure 12B is a profile along A-A' in figure 10C, the smoothed three-dimensional model. Figure 12C is the model from figure 6E with the real topography superimposed. Erosion is simulated by removing those parts of the model that protrude above the topography, and sedimentation is simulated by filling voids where the model surface is below the real surface. The three-dimensional and two-dimensional models are in substantial agreement and are consistent with the observed morphology and much of what is known or assumed about the geologic structure of the Yucca Mountain region.

Conclusions

With the help of boundary element models, the sets of parameters that reasonably reproduce observed tectonics have been identified. During the course of modeling we have reached the following conclusions:

- Detachment faulting is not required to explain the evolution of Yucca Mountain.
- Faults can join (or split) at depth without altering the surface topography.
- To produce models of Yucca Mountain we had to assume that a west-dipping fault with a substantial throw lies beneath Crater Flat. We also had to assume that crustal attenuation has occurred to the west and east of the Yucca Mountain region. Less likely alternatives are that the whole of Yucca Mountain has been lifted by volcanic underplating, or that there was pre-existing topography.
- Lacking more regional information, it is not possible to create a completely unambiguous model of the shear components of deformation around Yucca Mountain. However, the model that best approximates the observed deformation has more shear entering the region from the northwest than from the southeast.
- All block rotation models imply complex deformation in the region of the pivots. This should be observed at the north and south end of the main faults.
- Oroclinal bending is a feature of all of the rotating-block/beam-bending models. However, to replicate the observed increase of bending from north to south we must either extend the structures a long distance south below the sediments of the Amargosa Valley or assume extremely active pivots at the south end of the faulting.
- Yucca Mountain can be effectively modeled in three dimensions using the observed fault slips, a reasonable slip on the hypothesized Crater Flat fault, with the same assumptions as were needed for the two-dimensional model. A section across the three-dimensional model is in excellent agreement with the predictions of the two-dimensional model.

References Cited

- Crouch, S.L., and Starfield, S.L., 1983, Boundary element methods in solid mechanics: London, George Allen & Unwin.
- Ellis, M., and King, G.C.P., 1991, Structural control of flank volcanism in continental rifts: *Science*, v. 254, p. 839–842.
- Frizzell, V.A., Jr., and Shulters, Jacqueline, 1990, Geologic map of the Nevada Test Site, southern Nevada: U.S. Geological Survey Miscellaneous Investigations Map Series I-2046, scale 1:100,000.
- Gomberg, Joan, 1991, Seismicity and shear strain in the southern Great Basin of Nevada and California: *Journal of Geophysical Research*, v. 96, no. B10, p. 16383–16399.
- Hill, D.P., 1982, Contemporary block tectonics—California and Nevada: *Journal of Geophysical Research*, v. 87, no. B7.
- Jackson, J. A., 1987, Active normal faulting and crustal extension, *in* Coward, M.P., Dewey, J.F., and Hancock, P.L., eds., *Continental extensional tectonics*: Geological Society of America Special Publication 28.
- King, G.C.P., and Ellis, M., 1990, The origin of large local uplift in extensional regions: *Nature*, v. 348, p. 689–693.
- King, G.C.P., Stein, R., and Rundle, J., 1988, The growth of geological structures by repeated earthquakes—1, Conceptual framework: *Journal of Geophysical Research*, v. 93, no. B11, p. 13307–13318.
- Liggett, M.A., and Childs, J.F., 1974, Crustal extension and transform faulting in the southern Basin Range province: Report of Investigation, Argus Exploration Company.
- Lucchitta, Ivo, and Suneson, N.H., 1993, Dips and extension: *Geological Society of America Bulletin*, v. 105, p. 1346–1356.
- Massonet, D., Marc, R., Carmona, C., Adragna, F., Peltzer, G., Feigl, K., and Rabaute, T., 1993, The displacement field of the Landers earthquake mapped by radar interferometry: *Nature*, v. 364, p. 138–142.
- McKenzie, D., and Jackson, J., 1986, A block model of distributed deformation by faulting: *Journal of the Geological Society of London*, 143, p. 349–353.
- Nelson, M.R., and Jones, C.H., 1987, Paleomagnetism and crustal rotations along a shear zone, Las Vegas Range, southern Nevada: *Tectonics*, v. 6, no. 1, p. 13–33.
- Nur, Amos, Ron, H., and Scotti, O., 1986, Fault mechanics and the kinematics of block rotations: *Geology*, v. 14, p. 746–749.
- O'Neill J.M., Whitney, J.W., and Hudson, M.R., 1992, Photogeologic and kinematic analysis of lineaments at Yucca Mountain, Nevada; implications for strike-slip faulting and oroclinal bending: U.S. Geological Survey Open-File Report 91-623, 24 p.
- Ron, H., Aydin, A., and Nur, A., 1986, Strike-slip faulting and block rotation in the Lake Mead fault system: *Geology*, v. 14, p. 1020–1034.
- Rosenbaum, J.G., Hudson, M.R., and Scott, R.B., 1991, Paleomagnetic constraints on the geometry and timing of deformation at Yucca Mountain, Nevada: *Journal of Geophysical Research*, v. 96, no. B2, p. 1963–1979.
- Scott, R.B., 1990, Tectonic setting of Yucca Mountain, southwest Nevada, *in* Wernicke, B.P., ed., *Basin and Range extensional tectonics near the latitude of Las Vegas, Nevada*: Geological Society of America Memoir 176, p. 251–282.

- Scott, R.B., and Bonk, Jerry, 1984, Preliminary geologic map of Yucca Mountain, Nevada, with geologic sections: U.S. Geological Survey Open-File Report 84-494, scale 1:12,000.
- Stein, R., King, G.C.P., and Rundle, J., 1988, The growth of geological structures by repeated earthquakes—Two field examples of continental dip-slip faults: *Journal of Geophysical Research*, v. 93, no. B11, p. 13318–13324.
- Smith, R.B., and Bruhn, R.L., 1984, Intraplate extensional tectonics of the eastern Basin-Range—Inferences on structural style from seismic reflection data, regional tectonics, and thermal-mechanical models of brittle-ductile deformation: *Journal of Geophysical Research*, v. 89, no. B7, p. 5733–5762.
- Suppe, John, 1985, *Principles of structural geology*: Englewood Cliffs, N.J., Prentice-Hall, Inc., 537 p.
- Wernicke, Brian, and Axen, G.J., 1988, On the role of isostasy in the evolution of normal fault systems: *Geology*, v. 16, p. 848–851.
- Young, S.R., Stirewalt, G.L., and Morris, A.P., 1993, Geometric models of faulting at Yucca Mountain, *in* Housain, Q., ed., *Dynamic analysis and design considerations for high-level nuclear waste repositories*: Proceedings of American Society of Civil Engineers Symposium, San Francisco, Calif., 1992, American Society of Civil Engineers, New York.